Volume No.07, Issue No.03, March 2018 www.ijarse.com



Synthesis and Characterization of Mn/Polyaniline Nanocomposites via *in situ* approach

Harish Kumar^{1*}, Manisha¹

1. Dept. of Chemistry, Ch. Devi Lal University, Sirsa-125 055 (Haryana)

ABSTRACT

The wet chemical method was utilized for the synthesis of manganese nanoparticles. The conducting polymer polyaniline (PANI) was synthesized low temperature oxidative method. Mn-PANI nanocomposites was synthesized by in situ approach. The characterization of Mn-PANI nanocomposites was carried out by UV-Visible spectroscopy, FTIR, XRD and TEM techniques. The size of manganese nanoparticles observed from XRD and TEM techniques was 43.20 nm. The nanocomposites had cubic close packing with average particle size of 42.62 nm. The direct and indirect band gaps were calculated using UV-visible spectra data. Polymer nanocomposite exhibits superior properties such as mechanical, optical, electrical etc. as compared to microor macro-composites. Metal-polymer nanocomposites are used in the fields of ultrahigh/infralow refractive index materials, dichroic color filters, nonlinear optical filters, catalytic polymer membranes, etc.

Keywords: Manganese, Nanoparticles, Polyaniline, nanocomposites, conducting polymer.

I.INTRODUCTION

The modern concept of polymers as covalently bonded macromolecular structures was proposed in 1920 by Hermann Staudinger, who spent the next decade finding experimental evidence for this hypothesis [1]. Polyaniline (PANI) is a conducting polymer of the semi-flexible rod polymer family. It constitutes a large class of conducting polymers which are formed by the chemical or electrochemical oxidative polymerization of aniline or its derivatives [2]. Polyaniline (PANI) exists in a variety of forms that differ in chemical and physical properties [3-6].

A wide variety of nanocomposites can be prepared depending on the nature of the nanophase and the matrix [7,8]. A mixture of the beneficial properties were assumed by composite materials from their parent compounds which lead to the materials with improved physical properties and unprecedented flexibility.

Polymer-based composites were herald in the 1960s as a new concept for materials [9]. There are several approaches being reported to incorporate metal nanoparticles into polymers as polymers are the attractive matrix to imbibe nanoparticles [10]. The metal-polymer nanocomposites can be derived by combining properties from the parent constituents into a single material. Some new properties also have the possibilities to get generated which are unknown to parent constituent material [11]. Polymers nanocomposites supply materials that acquire the ease of processing with significantly improved and even multifunctional properties, opening the way to

Volume No.07, Issue No.03, March 2018

www.ijarse.com

ISSN: 2319-8354

absolutely new applications of polymers. Polymer nanoparticle composite whether in solution or in bulk, offer unique mechanical, electrical, optical and thermal properties [12].

To maximise the excellent properties of metal-polymer nanocomposites, we have synthesized manganese oxide/polyanilinenanocomposites by sol-gel technique and then they are characterized by using different techniques like UV-visible, FTIR, XRD, TEM techniques.

II.EXPERIMENTAL SECTION

Synthesis of Manganese oxide nanoparticles:

Following steps were used for the synthesis of nanoparticles of manganese by Sol-gel method: Acidified solution 'A' was prepared of metal salt. Solution 'B' was prepared of TEOS and ethanol. Both solutions were mixed with constant stirring. The solution was then heated at 70.0 °C with constant stirring. The container was kept closed undisturbed. The sol prepared was then filled into the previously sterilized petriplates. The temperature of these petriplates was maintained at 100.0 °C for 24.0 hours. Petriplates were watched for gelation and complete aging. The samples were annealed in muffle furnace maintained at temperature of 400°C for 4.0 hours.

Synthesis of Polyaniline:

Following steps were used for the synthesis of polyaniline by chemical polymerization method.50.0ml distilled monomeric solution was taken then SLS (sodium lauryl sulphate) and acidic FeCl₃ were added with constant stirring and 5-7°C temperature was maintained. Reaction mixture was stirredcontinuously till thick dark solution was obtained which was then filtered under suction pump and then washed with acetone and dried at 100.0 °C.

Synthesis of in situ Manganese oxide-PANI nanocomposites:

Following steps were used for the *in* situ synthesis of Mn/PANInanocomposites.50.0 ml distilled monomer was taken and SLS was added maintaining low temperature. Another solution of acidic metal nanoparticles was prepared and acidic FeCl₃ was added and the solutions were mixed with constant stirring, filtered, washed with acetone and dried at 100.0 °C.

III.CHARACTERIZATION

UV-Visible spectroscopic Analysis:

Figure 1 shows UV-visible spectra of Mn_2O_3 nanoparticles as a function of wavelength. The UV-Visible absorption spectroscopy of Mn_2O_3 nanoparticles shows an absorption peak at about 339.60 nm. Figure 2(a) is the Tauc plot showing variation of $(\alpha h \nu)^{1/2}$ vs. hv and Figure 2(b) is the Tauc plot showing variation of $(\alpha h \nu)^2$ vs. hv. These plots are calculated from UV-visible spectra for manganese oxide nanoparticles synthesized by Sol-gel technique. The direct and indirect band gap (Eg) of manganese oxide nanoparticles corresponding to absorption peak at 339.60 nm was found to be 2.5 and 2.6 eV, respectively.

Volume No.07, Issue No.03, March 2018

www.ijarse.com



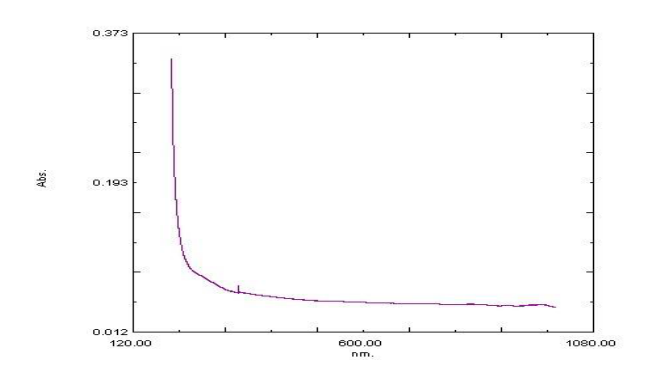


Figure 1 UV-Visible absorption spectra of manganese oxide nanoparticles synthesized by Sol-gel technique.

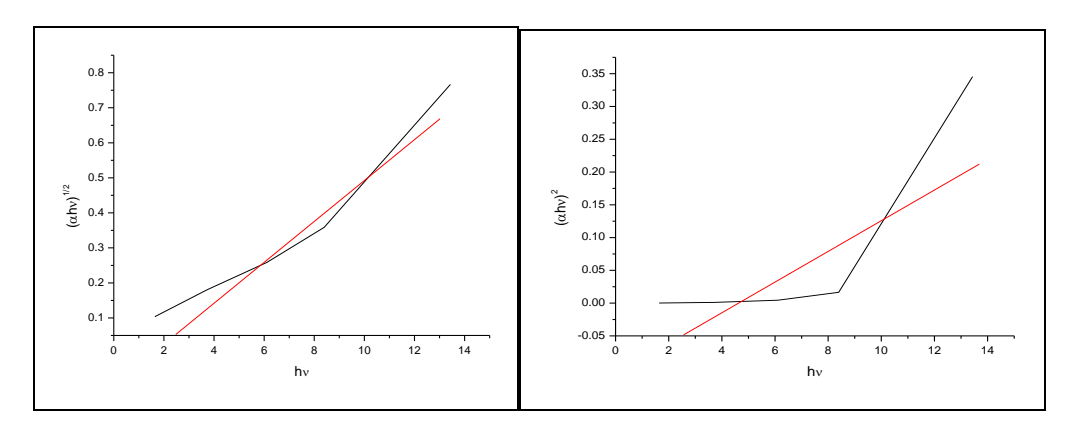


Figure 2(a) Tauc plot of $(\alpha hv)^{1/2}$ vs. hv. Figure

Figure 2(b) Tauc plot of $(\alpha h v)^2 vs. h v$

FTIR Spectroscopic Analysis:

Figure 3 illustrate the FTIR spectra of manganese oxide nanoparticles synthesized by Sol-gel technique. The absorption peaks at 644, 617, 574 and 436 cm⁻¹ correspond to the characteristic Mn-O stretching vibration mode of Mn_2O_3 . The band at 3425 cm⁻¹ is due to O-H stretching vibration and a band at 1604.77 cm⁻¹ is assigned H-O-H bending vibration of adsorbed water molecule. The presence of both of these peaks indicated the existence of adsorbed H₂O molecule for this sample. Furthermore, the absorption peak at the wavelength near 1080 and 791 cm⁻¹ may be due to -OH groups of Mn-OH for manganese oxide nanoparticles.

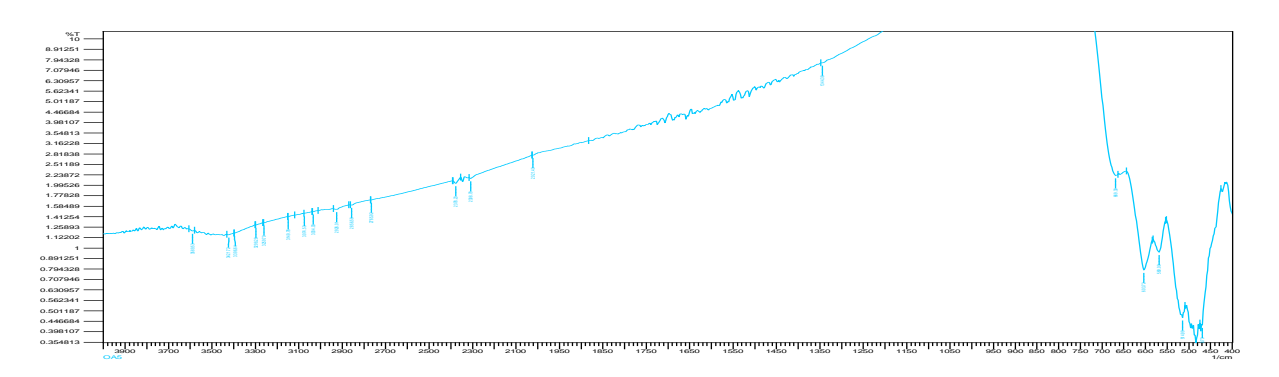


Figure 3 FTIR spectra of manganese oxide nanoparticles synthesized by Sol-gel technique.

Volume No.07, Issue No.03, March 2018

www.ijarse.com

IJARSE ISSN: 2319-8354

XRD Analysis:

Figure 4 show the XRD pattern of manganese oxide nanoparticles synthesized by Sol-gel technique. The X-ray Diffraction pattern reveal major peaks at 2θ values of 23.35 (211), 33.14 (222), 38.45 (400), 45.34 (332) and 49.49 (431), respectively. All the diffraction peaks of the sample correspond to α - Mn_2O_3 nanoparticles (space group Ia3(206)) with lattice constants a = b = c = 9.40 A°, which are in agreement with the reported values of JCPDS card no. 41-1442 and 71-0636. The XRD pattern identifies the given sample as Mn_2O_3 with cubic structure. Average particle size of the manganese oxide nanoparticles corresponding to the highest intensity peak was found to be 29.61 nm using Debye Scherrer formula ($d = K \lambda / \beta cos\theta$).

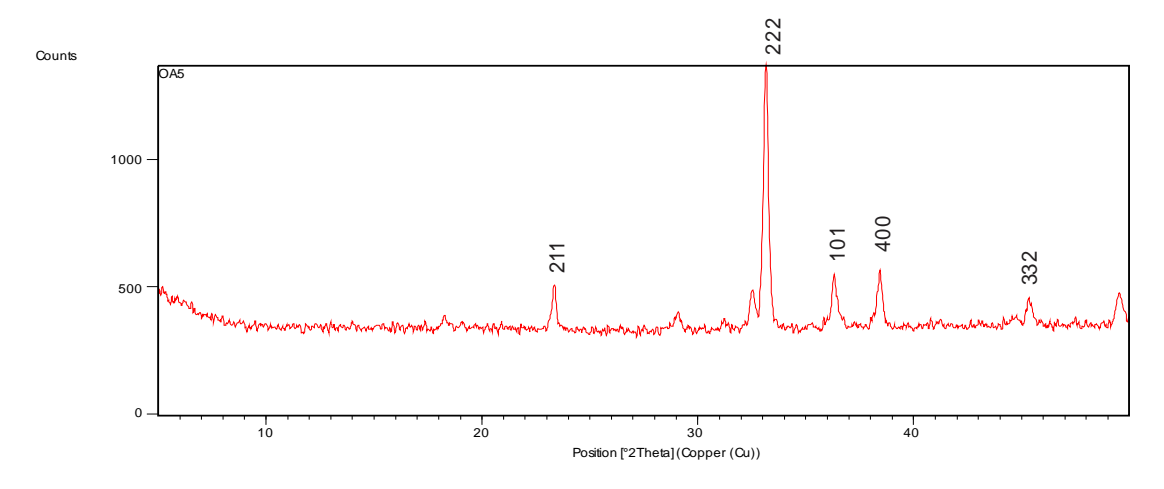


Figure 4 XRD pattern of manganese oxide nanoparticles synthesized by Sol-gel technique.

TEM Analysis:

Figure 5 shows the TEM image of the $\rm Mn_2O_3$ nanoparticles synthesized by sol-gel method. The microstructural characterization was conducted to determine the size of nanoparticles and to examine the homogeneity and size distribution. The particles observed to be spherical shape. It can be seen from the Figure 5 that there is a uniform distribution of particle with mean particle size 21.5 nm.

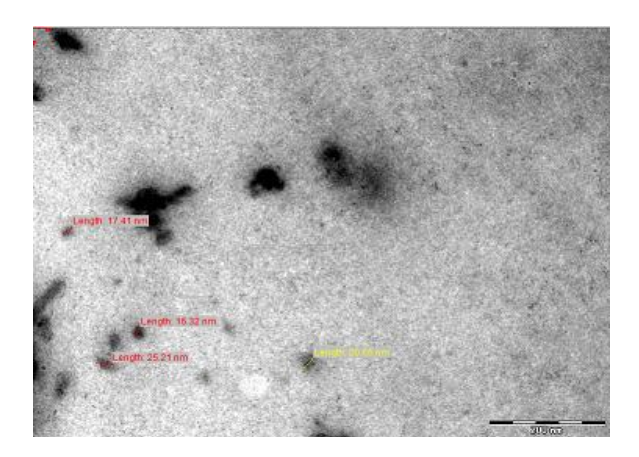


Figure 5 TEM image of manganese oxide nanoparticles synthesized by Sol-gel technique.

Volume No.07, Issue No.03, March 2018

www.ijarse.com



Polyaniline:

Polyaniline (PANI) is an important conducting polymer due to its facile synthesis, environmental stability, and controllable physical and electrochemical properties by oxidation and protonation. PANI has been used in cathode materials of the lithium-ion secondary storage batteries.

UV-Visible absorption spectroscopic analysis:

Figure 6 shows the UV-visible spectra of polyaniline as a function of wavelength. The UV-visible spectra shows absorption peak at 329 nm. Figure 7(a) is the Tauc plot showing variation of $(\alpha hv)^{1/2}$ vs. hv and Figure 7(b) is the Tauc plot showing variation of $(\alpha hv)^2$ vs. hv. These plots were calculated from UV-visible spectra for polyaniline nanoparticles synthesized by oxidative polymerization method. The direct and indirect band gap (Eg) of polyaniline nanoparticles corresponding to absorption peak at 329 nm was found to be 3.44 and 3.49 eV, respectively. It is clear from band gap that the synthesized polyaniline are of semiconductor type.

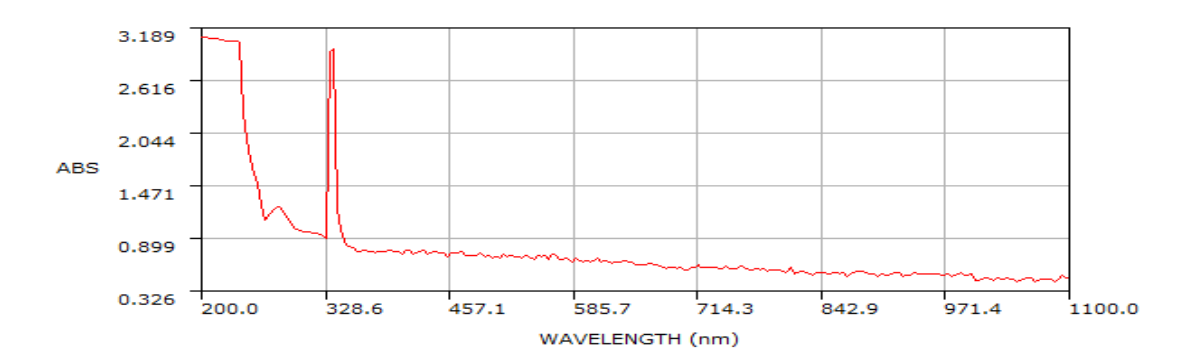


Figure 6 UV-Visible absorption spectra of polyaniline.

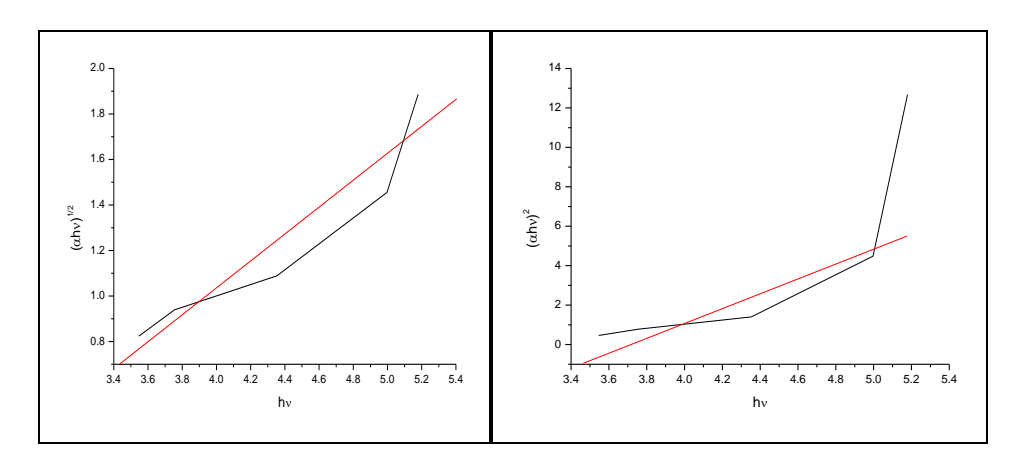


Figure 7(a) Tauc plot $(\alpha hv)^{1/2}$ vs. hv Figure 7(b) Tauc plot $(\alpha hv)^2$ vs. hv

Volume No.07, Issue No.03, March 2018

www.ijarse.com



FTIR Analysis:

Figure 8 shows FTIR spectra of polyanilinenanocomposite. The absorption peak at 3410 cm⁻¹ is due to –OH group of adsorbed water molecules. The distinctive peaks at 1580 and 1500 cm⁻¹ match to the quinoid ring and the benzene ring, respectively (Figure 8). The bands in the range 1200–1400 cm⁻¹ correspond to the C–N stretching band of an aromatic amine. The typical band of polyaniline base (N=Q=N stretching band) was observed at 1130 cm⁻¹. The bands close to 820 cm⁻¹ are characteristic of the p-substituted chains of polyaniline. The band close to 1145 cm⁻¹ is described as being characteristic of the conducting polymer due to the delocalization of electrical charges caused by deprotonation and it can be attributed to bands characteristics of B-NH-Q or B-NH-B (where B refers to the benzenic-type rings and Q to the quinonic-type rings). In the region close to 1300 cm⁻¹, the peaks are attributed to the presence of aromatic amines present in all types of polyaniline. The intensity of these bands gives an idea of the oxidation state of polyaniline when they present similar intensities; the polyaniline is in the emeraldine form.

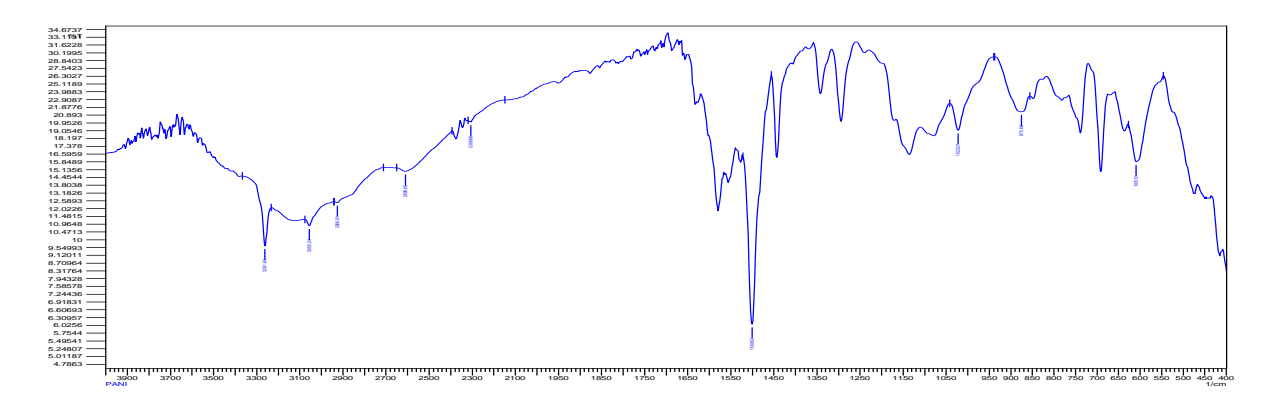


Figure 8 FTIR spectra of conducting polymer polyaniline.

XRD Analysis:

Polyaniline is semicrystalline or of amorphous nature as reported by different researchers. Polyaniline crystallizes in the monoclinic space group P21. The diffraction pattern (Figure 9) shows a well-developed crystallinity in the sample prepared at 4.0 0 C. Diffraction peaks were obtained at $2\theta = 40$ (100), 180 (210), 20.50 (310) and 220 (311). The crystallite size (d) of the material of thin film has been evaluated by Scherrer's formula. The crystallite size of polyaniline conducting polymer was 44.20 nm.

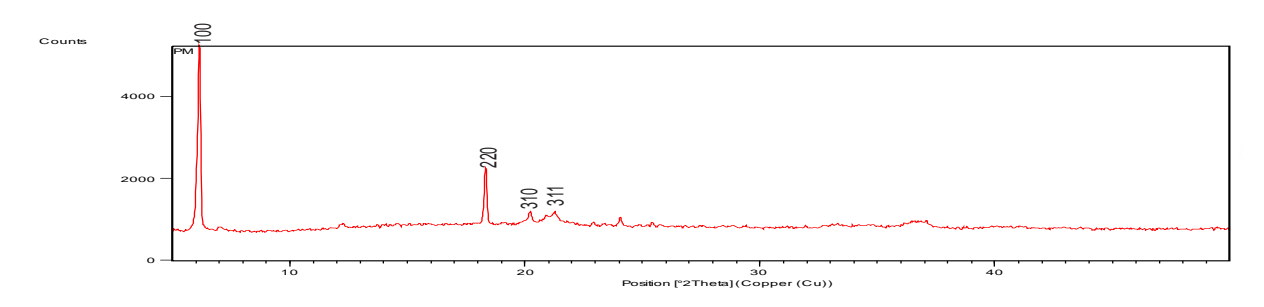


Figure 9. X-ray diffraction pattern of polyaniline.

Volume No.07, Issue No.03, March 2018

www.ijarse.com

ISSN: 2319-8354

TEM Analysis:

The needle-shaped or nano-web structures are seen in TEM image of polyaniline (Figure 10). The surface of polyaniline nanoparticles is quite smooth and those are well dispersed. Average particle size of polyaniline was observed to be 30.0 nm.

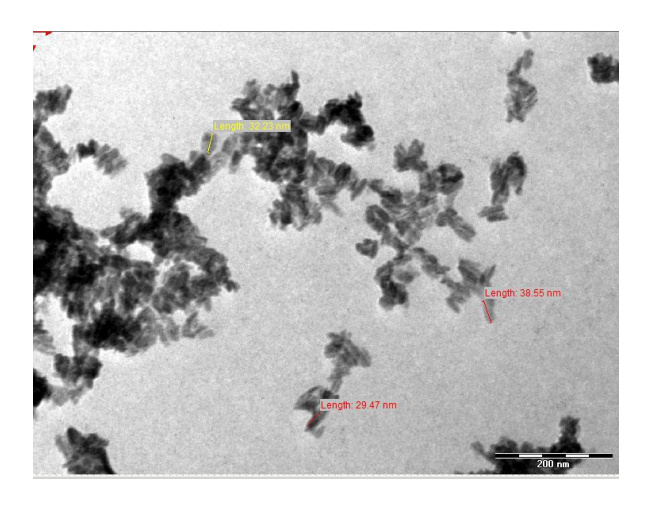


Figure 10.TEM image of conducting polymer polyaniline.

Mn/PANI Nanocomposites (in situ):

UV-Visible Analysis:

Figure 11 shows the UV-visible absorption spectra of Mn/polyaniline as a function of wavelength. The UV-visible spectra shows band at 328.6 nm. Figure 12(a) is the Tauc plot showing variation of $(\alpha hv)1/2$ vs. hv and Figure 12(b) is the Tauc plot showing variation of $(\alpha hv)2$ vs. hv. These plots are calculated from UV-visible spectra for Mn/PANI nanocomposites synthesized by *in situ* method. The direct and indirect band gap (Eg) of Mn/PANI nanoparticles corresponding to absorption peak at 328.6 nm was found to be 2.55 and 2.85 eV, respectively. It is clear from band gap that the synthesized Mn/polyaniline is of semiconductor type.

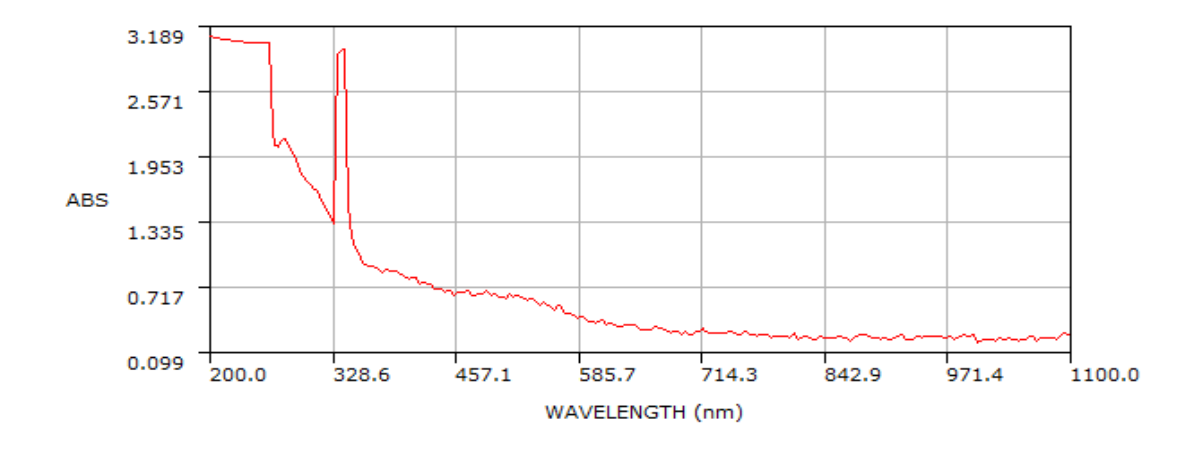


Figure 11 UV-visible absorption spectra of Mn/PANI (in situ) nanocomposites.

Volume No.07, Issue No.03, March 2018

www.ijarse.com



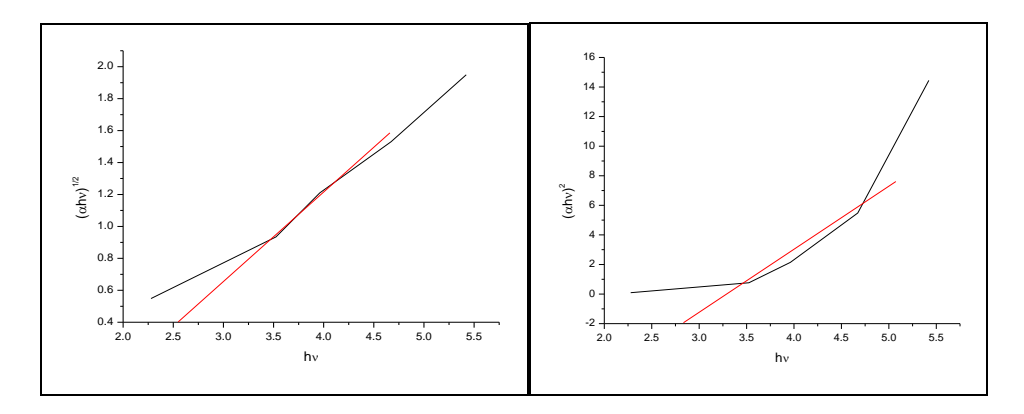


Figure 12(a) Tauc plot $(\alpha h v)^{1/2}$ vs. hv

Figure 12(b) Tauc plot $(\alpha h v)^2$ vs. hv

FTIR Analysis:

Figure 13 shows the FT-IR spectra of Mn/PANInanocomposite. A band in the range of 1,600 to 1,000 cm⁻¹ which comes from the vibrational and rotational bands of the functional groups in PANI. The bands at 1,568 and 1,495 cm⁻¹ can be assigned to C=C stretching of quinoid and benzenoid rings; the C-N stretching for the benzenoid unit appear at 1,297 and 1,239 cm⁻¹, respectively. The peak at 1,144 cm⁻¹ can be attributed to the inplane bending vibration of aromatic C-H. The weak band at 3,320 cm⁻¹ is attributed to N-H stretching. The FT-IR spectra obtained from PANI/MnO₂nanocomposite showed characteristic peaks of PANI (Figure 13). For example, vibrational peaks cantered at 1,565 and 1,468 cm⁻¹ are attributed to the stretching peaks of quinoid and benzenoid deformations of PANI. We also observed C-N stretching peaks at 1,238 and 1,300 cm⁻¹ and C-H bending of protonated PANI at 1,124 cm⁻¹. The band in the regions over 400 cm⁻¹ can be assigned to Mn-O stretching vibrations. FT-IR spectra of the PANI/MnO₂nanocomposite are similar to those of PANI, but the bands' characteristic of polymer backbone at 1,500 and 1,600 cm⁻¹ are shifted to higher values after annealing, indicating deprotonation. The peak at 1,195 cm⁻¹ is suppressed after annealing to a greater extent for PANI compared to that for the nanocomposites, indicating a higher extent of deprotonation in pure PANI compared to nanocomposites. The results of FT-IR spectra confirm the presence of both components in the nanocomposite.

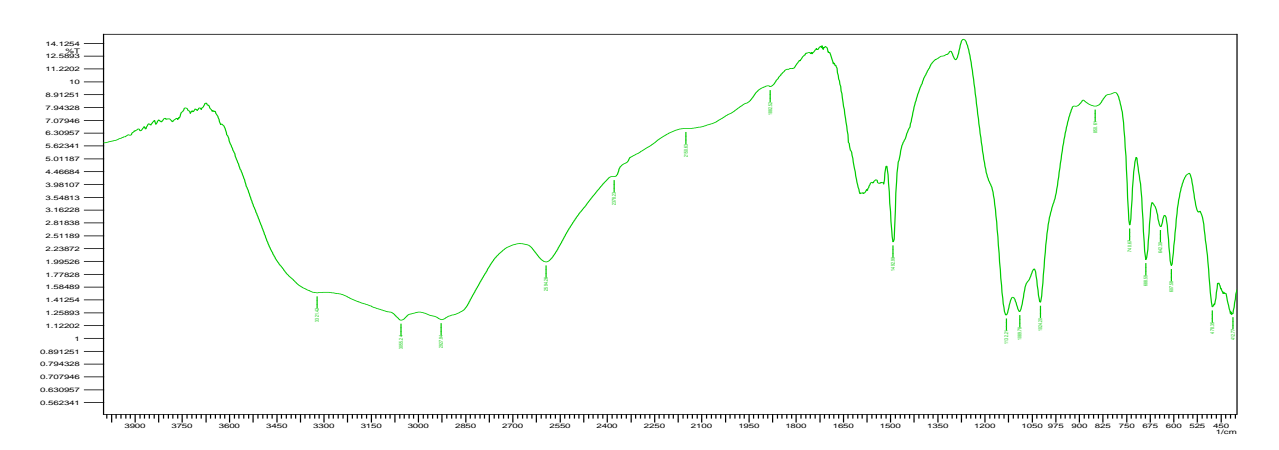


Figure 13. FTIR spectrum of Mn/PANI (in situ) nanocomposites.

Volume No.07, Issue No.03, March 2018

www.ijarse.com

IJARSE ISSN: 2319-8354

XRD Analysis:

The diffraction pattern of PANI/MnO₂ (Figure 14) shows a well-developed crystallinity in the sample prepared at 4.0° C. Diffraction peaks were obtained at $2\theta = 3.70(100)$, 18.00 (220), 20.50(310), 22.00(311) and 25.50(321). The diffraction peak at $2\theta = 25.50$ (321) is due to PANI/MnO₂nanocomposite. The crystallite size (d) of the material of thin film has been evaluated by Scherrer's formula and is found to be 43.20 nm.

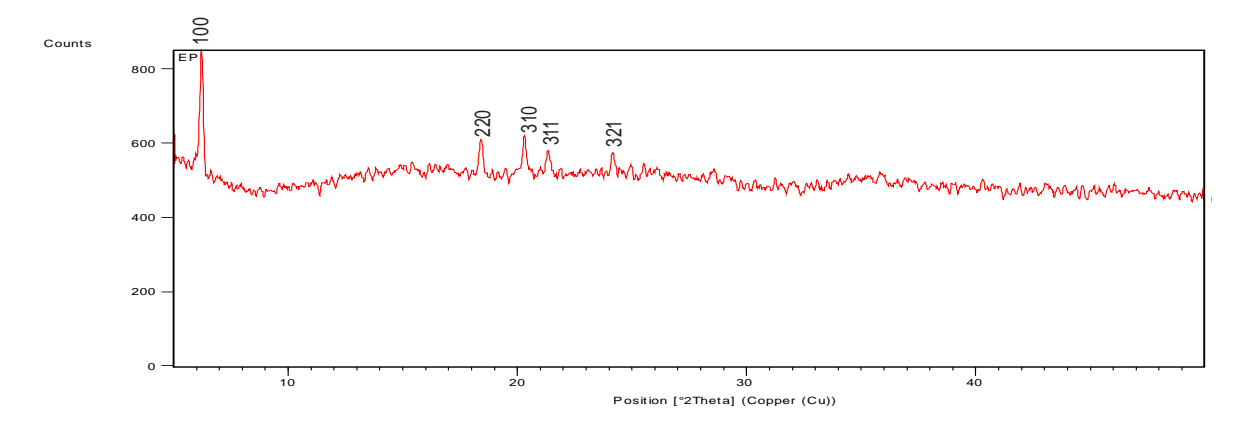


Figure 14 X-ray diffraction pattern of Mn/PANI (in situ) nanocomposites.

TEM Analysis:

Morphologies of the nanocomposites were examined using TEM techniques. Rod-shaped Mn/PANI nanocomposites are observed as shown in Figure 15. Average particle size as observed from TEM image was 40.0 nm.

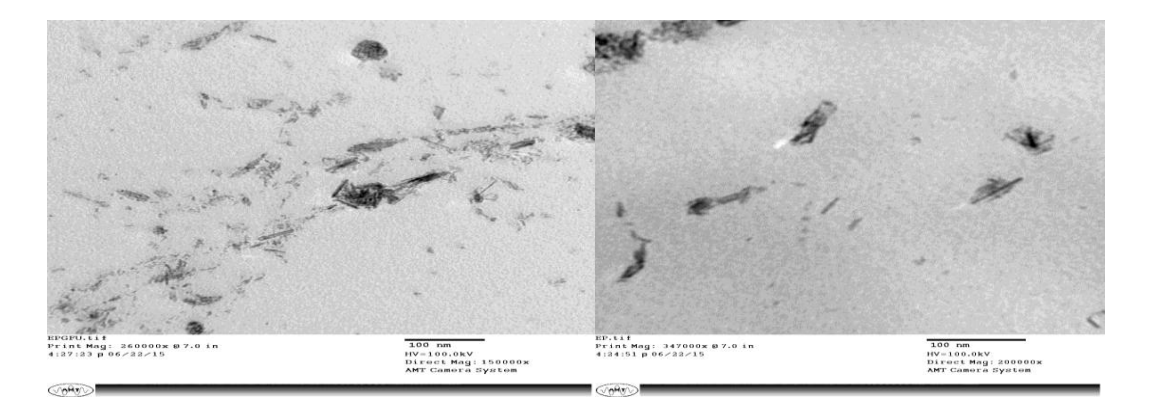


Figure 15 TEM images of Mn/PANI (in situ) nanocomposites.

IV.CONCLUSION

The average particles size, shape and morphology of the manganese oxide nanoparticles was determined by UV-visible, FT-IR spectroscopy, XRD and TEMtechniques. The diffraction pattern of manganese oxide nanoparticles synthesized by sol-gel technique corresponds to α -Mn₂O₃ nanoparticles with cubic structure. The

Volume No.07, Issue No.03, March 2018

www.ijarse.com

IJAKSE ISSN: 2319-8354

average size of the manganese oxide nanoparticles was found to be 29.61 nm. The mean size of the spherical and non-spherical manganese oxide nanoparticles synthesized by sol-gel and TEMtechnique was found to be 21.5 nm and 25.6 nm, respectively. The sizes of manganese oxide nanoparticles found by TEM analysis are in close agreement with the XRD analysis.FTIR absorption bands reveal the information about purity and nature of chemical environment of metal nanoparticles. The diffraction pattern of conducting polymer polyaniline corresponds to its crystalline nature with average particle size of 44.20 nm. The TEM analysis of polyaniline reveals the needle-shaped or nano-web structures with the mean size of 30.0 nm. The diffraction pattern of Mn/PANI nanocomposites synthesized by *in situ* method showed the well-developed crystalline nature with the average particle size of 43.20 nm, respectively.The TEM image analysis of Mn/PANI nanocompositessynthesized by *in situ* method revealed the rod-shape with average particle size of 40.0 nm.

REFERENCES

- 1.Allcock, R. Harry, Lampe, W. Frederick, Mark, E. James, Contemporary Polymer Chemistry (3rd), PearsonEducation, p. 21, 2003
- 2. A. G. MacDiarmid, A. J. Epstein, Faraday Discuss. Chem. Soc., 88, 317, 1989
- 3.Okamoto, Yoshikuko and Brenner, Walter, "Polymer" Ch. 7, pp. 125-158 Inorganic Semiconductors, Reinhold, 1964
- 4. J. Stejskal, P. Kratochirl, A. D. Jenkins, Polymer, 37, 367, 1996
- 5.D. C. Trivedi, In Handbook of Organic Conductive Molecules and Polymers, H. S. Nalwa (Ed.), 2, 502-572, Wiley, Chichester, 1997
- 6. N. Gospodinova and L. Terlemezyan, Prog. Polym.Sci, 23, 1443, 1998
- 7.P.M. Ajayan et al., NanocompositeSci& Tech, 230, 2005
- 8. J. Kim and B. Vander Bruggen, "The use of nanoparticles in polymeric and ceramic membrane structures: Review of manufacturing procedures and performance improvement for water treatment", Environment Pollution, 158(7), 2335-2349, 2010
- 9. T. Ramanathan, A. A. Abdala, S. Stankovich, D. A. Dikin, M. Herrera-Alonso, R. D. Piner, et al., "Functionalized graphene sheets for polymer nanocomposites", Nature Nanotech, 3, 327-331, 2008
- 10. F. Faupel, V. Zaporojtchenko, H. Greve, U. Schurmann, H. Takele, C. Hanisch, "Metal-Polymer Nanocomposites for Functional Applications", Adv. Engg. Mat, 12(12), 1177-1190, 2010
- 11. S. P. Gubin, "Metal containing nano-particles withinpolymeric matrices: preparation, structure and properties", Colloids & Surfaces, 202, 155-163, 2002
- 12. A. Usuki, M. Kato, A. Olada, T. Kurauchi, "Synthesis of Polypropylene-Clay Hybrid", J. Appl. Polym. Sci., 63, 137, 1997